

Polysomes-Mediated Delivery of CSF1R Inhibitor to Tumor Associated Macrophages Promotes M2 to M1-Like Macrophage Repolarization

Manuel Rodriguez-Perdigon,* Sèuhn Jimaja, Laetitia Haeni, Nico Bruns, Barbara Rothen-Rutishauser, and Curzio Rüegg

The crosstalk between cancer cells and tumor associated macrophages (TAMs) within the tumor environment modulates tumor progression at all stages of cancer disease. TAMs are predominantly M2-like polarized macrophages with tumor-promoting activities. Nonetheless, they can be repolarized to tumoricidal M1-like macrophages through macrophage colony stimulating factor 1 receptor inhibition (CSF1Ri). CSF1Ri is being explored as multifaceted therapeutic approach to suppress TAMs tumor-promoting functions and reduce cancer cell aggressiveness and viability. However, treatment with CSF1Ri results in significant TAMs death, thereby extinguishing the possibility of generating tumoricidal M1-like macrophages. Immunotherapy has not only improved overall patient's survival in some cancer types, but also caused frequent off-target toxicity. Approaches to balance efficacy versus toxicity are needed. Herein, a CSF1Ri-loaded polysomes (PMs) based delivery platform is developed to promote M2-like macrophage repolarization. When testing in vitro on primary human monocyte-derived macrophages (MDMs), CSF1Ri-loaded PMs are preferentially taken up by M2-like macrophages and enhance M2 to M1-like macrophage repolarization while minimizing cytotoxicity in comparison to the free drug. When testing in a MDMs-MDA-MB-231 breast cancer cell coculture model, CSF1Ri-loaded PMs further retain their M2 to M1-like macrophages polarization capacity. This CSF1Ri-loaded PM-based platform system represents a promising tool for macrophage-based immunotherapy approaches.

1. Introduction


Macrophages are crucial players of the innate and adaptive immune system. They also actively partake in promoting cancer progression, from the stage of early neoplastic transformation to metastasis formation and therapy resistance.^[1,2] Macrophages are present in the tumor environment in high numbers as tissue resident macrophages or upon local differentiation from blood circulating monocytes recruited to the tumor.^[3] Tumor-associated macrophages (TAMs) may account for up to 50% of the tumor cell mass.^[4-6] In most tumors, their density positively correlates with tumor growth, invasion and metastasis, and is associated with poor patients' prognosis.^[5,7-10]

Macrophages have shown great heterogeneity and functional plasticity depending on the tissue microenvironment stimuli encountered.^[11,12]

They can typically acquire two divergent phenotypes: M1-like macrophage with proinflammatory and tumoricidal properties, and M2-like macrophages with anti-inflammatory, immunosuppressive, and tumor-promoting properties.^[13-18]

M. Rodriguez-Perdigon, C. Rüegg
Department of Oncology
Microbiology and Immunology
Faculty of Science and Medicine
University of Fribourg
Chemin du Musée 18, PER17, Fribourg 1700, Switzerland
E-mail: manuel.rodriguez@unifr.ch

S. Jimaja, L. Haeni, N. Bruns, B. Rothen-Rutishauser
Adolphe Merkle Institute
University of Fribourg
Chemin des Verdiers 4, Fribourg 1700, Switzerland
N. Bruns
Department of Pure and Applied Chemistry
University of Strathclyde
Thomas Graham Building
295 Cathedral Street, Glasgow G1 1XL, UK

 The ORCID identification number(s) for the author(s) of this article can be found under <https://doi.org/10.1002/mabi.202200168>

© 2022 The Authors. Macromolecular Bioscience published by Wiley-VCH GmbH. This is an open access article under the terms of the Creative Commons Attribution License, which permits use, distribution and reproduction in any medium, provided the original work is properly cited.

DOI: 10.1002/mabi.202200168

TAMs promote tumor progression by stimulating tumor cell survival, growth, invasion, and tumor angiogenesis, inhibiting the immune response and favoring metastasis.^[3,19] Because of their tumor promoting role, TAMs are being considered as potential and promising therapeutic targets for anticancer therapies.^[20,21] Shaping this macrophage plasticity toward an antitumor phenotype by using versatile and stable drug delivery systems can unlock a huge potential in developing safe and efficacious combinatorial cancer immunotherapies.^[22]

Macrophage colony-stimulating factor 1 (M-CSF1) plays crucial roles in macrophages production, differentiation, and survival.^[23,24] M-CSF1 induced cellular activities are mediated by the tyrosine kinase transmembrane receptor CSF1R activating the RAS-RAF-MAPK and PI3K-AKT signaling pathways.^[25] Within a tumor context, M-CSF1 is secreted by tumor cells and acts as an important promoter of mammary tumor progression to metastasis by enhancing infiltration, survival and proliferation of M2-like macrophages. Among the different breast cancer subtypes, triple negative breast cancer (TNBC) has been shown to express low levels of both M-CSF1 and CSF1R. Thus, the crosstalk between this cancer subtype and TAMs form both autocrine and paracrine signaling loops that promote tumor formation, progression, and evasion of apoptosis.^[26,27] Because this paracrine signaling loop is independent on CSF1R expression in tumor cells, blocking M-CSF1R signaling in TAMs represents an attractive strategy to deplete and, most importantly, repolarize the M2-like macrophages toward a more tumoricidal M1-like phenotype. This concept has been translated into the clinics, and several clinical trials targeting M-CSF1/CSF1R axis are in progress or completed for a number of different cancer types, including melanoma, lymphoma, leukemia, glioblastoma, prostate, pancreatic, and colorectal cancers.^[28–30] Current approaches to block CSF1R signaling with CSF1R inhibitors (CSF1Ri) is based on the development of small molecules and monoclonal antibodies targeting the intracellular kinase or the extracellular ligand-binding domains, respectively.^[31,32] Both small molecules and monoclonal antibodies approaches in monotherapy have prolonged the survival of cancer patients with diffuse-type tenosynovial giant cell tumors,^[28,33] whereby 39% of the patients responded completely to the small molecule CSF1Ri pexidartinib versus 0% patients that received placebo.^[34] For most other types of cancers, however efficacy is still limited. Although blocking the M-CSF1/CSF1R axis exhibited a rather favorable safety profile in monotherapy, frequent off-target toxicity events (e.g., hepatotoxicity, edema, gastrointestinal or skin related side effects) have been observed, depending mainly on the type of tumor and its location, CSF1R tumor expression, and tumor-type specificities of TAMs.^[28,35]

Typically, anticancer drugs are given as free drugs, but because of poor drug solubility, limited bioavailability, high clearance, or impaired penetration to the tumor site, the therapeutic index is often unfavorable.^[36] To address this issue, approaches to improve drug delivery have been proposed and explored, including those based on nanoparticles, and different drug development strategies have been tested.^[37–40] One common limiting factor of traditional encapsulating delivery systems, however, is their limited drug loading capacity and long-term stability, potentially impairing practical applications. Polymersomes (PMs), e.g., block copolymer vesicles, have great potential as

Table 1. Treatment of the M2-like macrophages repolarization and uptake of PMs during 2 days (abbreviations: fluorescein, FLN; M2-like macrophage stimulation culture medium, sM2).

Sample description	Macrophage repolarization conditions	Macrophage uptake of PMs conditions
Untreated	sM2	sM2
Vehicle (VH)	sM2 with VH ^{a)}	sM2 with VH ^{a)}
Free CSF1Ri	sM2 with 10 μ m CSF1Ri	sM2 with 10 μ m CSF1Ri
Empty PMs	sM2 with empty PMs ^{b)}	sM2 with FLN-loaded PMs ^{b)}
CSF1Ri-PMs	sM2 with CSF1Ri-PMs	sM2 with CSF1Ri-FLN PMs

^{a)}As CSF1Ri (BLZ945) negative control, equal volumes of vehicle solution (VH) (1:3 mixture of THF/H₂O v/v) solution was added; ^{b)}As CSF1Ri-loaded PM (CSF1Ri-PMs) negative control, equal volume of empty PMs was added.

drug-delivery vehicles because of their stability and tuneability.^[41] Indeed, the various possibilities for their functionalization and surface-modification offer routes toward tunable and targeted drug-delivery systems.^[42–44]

Here, we developed and tested a novel drug delivery platform consisting of PM encapsulating the CSF1Ri small molecule 4-[[2-[[[(1R,2R)-2-hydroxycyclohexyl]amino]-6-benzothiazolyl]oxy]-N-methyl-2-pyridinecarboxamide (BLZ-945), to promote M2 to M1-like macrophage repolarization using monocyte-derived macrophages (MDMs). We show that \approx 400 nm diameter CSF1Ri-loaded PMs a) are preferentially uptaken by M2-like macrophages compared to M1-like macrophages, b) efficiently repolarize macrophage from M2 to M1-like phenotype, and c) are less cytotoxic to macrophages compared to free drug resulting in a higher number of repolarized M1 macrophages. When tested in a macrophage-TNBC coculture model, sustained CSF1R inhibition by drug-loaded PMs retained the M2 to M1-like repolarization effect, without causing significant macrophage apoptosis.

Taken together, this study shows that sustained CSF1Ri blockade by versatile and effective drug encapsulation in PMs can promote M2 to M1-like macrophage repolarization without causing significant death. These results are of potential interest for use in combination with other antitumor immunotherapy approaches.

2. Results and Discussion

2.1. CSF1Ri-Loaded Polymersomes Are Taken Up by Macrophages

First, we assessed the ability of human M2-like macrophages to internalize drug-loaded or empty PMs. PMs of a poly(ethylene glycol)-*block*-poly(hexyl methacrylate) (PEG-*b*-PHMA) diblock copolymer were prepared by solvent exchange. PEG was chosen as it is a hydrophilic polymer that provides stealth properties to PMs. PHMA was chosen as the hydrophobic block because it forms flexible and fluidic PMs membranes.^[45] The characterization of the PMs is shown in Figures S1–S4 of the Supporting Information and **Tables 1** and **2**.

Primary human MDMs were polarized to an M2-like activation state after M-CSF1, interleukins (IL) IL-4, IL-10, and IL-13 (Figure S5, Supporting Information). These cytokines

Table 2. Treatment of MDA-MB-231 from monocultures and M2-like macrophages from cocultures (abbreviation: M2-like macrophage stimulation culture medium, sM2).

Sample description	5 days monocultures conditions	5 days indirect coculture conditions
Untreated	cRPMI	sM2
Vehicle (VH)	cRPMI with VH ^{a)}	sM2 with VH ^{a)}
Free CSF1Ri	cRPMI with CSF1Ri	sM2 with CSF1Ri
Empty PMs	cRPMI with empty PM ^{b)}	sM2 with empty PM ^{b)}
CSF1Ri-PMs	cRPMI with CSF1Ri-PMs	sM2 with CSF1Ri-PMs

^{a)}As CSF1Ri (BLZ945) negative control, equal volumes of vehicle solution (VH) (1:3 mixture of THF/H₂O v/v) solution was added; ^{b)}As CSF1Ri-loaded PMs negative control, equal volume of empty PMs was added.

are responsible for the generation of M2a and M2c polarized macrophage subsets whose phenotypes are associated with anti-inflammatory, tissue remodeling, proangiogenic, and tumor-promoting activities.^[46] MDMs have been proved to better reflect effective response of immunomodulators compared to widely used murine macrophage in vitro models (e.g., RAW264.7).^[47] M2-like macrophages were treated for 48 h with either PMs loaded with both fluorescein (FLN as a fluorescent tracer) and CSF1R kinase inhibitor (CSF1Ri) BLZ-945 at 8.5×10^{-6} M of drug concentration (CSF1Ri-FLN loaded PMs); PMs loaded with only fluorescein (FLN-loaded PMs); free CSF1Ri at 10×10^{-6} M or vehicle (VH) (1:3 mixture of tetrahydrofuran (THF)/H₂O v/v). As shown in **Figure 1a,c**, we found a significantly higher content of CSF1Ri-FLN loaded PMs in M1-like macrophages (CD11b⁺CD86⁺) compared to the empty PMs (e.g., drug free). Conversely, we observed a trend toward a higher uptake of empty PMs by M2-like macrophages (CD11b⁺CD206⁺) versus M1-like macrophages (CD11b⁺CD86⁺) (**Figure 1a,b**). This is consistent with an efficient uptake of CSF1Ri-FLN loaded PMs by M2-like macrophages, which have higher phagocytic capacity,^[48,49] and polarization toward M1-like macrophages. Treatment with free CSF1Ri, as expected, did not cause an increase in green (FLN) fluorescence intensity (**Figure 1a**). As CSF1Ri-loaded PMs educate M2-like macrophages to become M1-like macrophages, this results in higher CSF1Ri-loaded PMs content in the M1-like macrophages (CD11b⁺CD86⁺) at the end of the 48 h treatment. This CSF1Ri-FLN loaded PMs internalization was further validated in situ by confocal microscopy imaging. After CSF1Ri-FLN loaded PM (8.5×10^{-6} M of drug concentration) incubation of M2-like macrophages for 4, 12, and 24 h (**Figure 1d**), we confirmed a PMs internalization at 4 h incubation by XY profile fluorescence mean intensity analysis of confocal images (**Figure S6**, Supporting Information). Additionally, we noticed an increasing rounded morphology of the macrophages at 12 and 24 h (**Figure 1d**), consistent with an M2 to M1-like macrophage repolarization over time.^[50] We encapsulated CSF1Ri into ≈ 400 nm diameter PMs. This range of PMs diameter represents 50-fold lower size than the average diameter of a macrophage (20 μ m), which implies a high-volume burden for these phagocytic cells. We still observed that M2-like macrophages take up ≈ 400 nm diameter drug-loaded PMs after 4 h of incubation and respond to their cargo (CSF1Ri) over 12 h of treatment (**Figure 1d**). For example, particle size ranging from 20 nm to 1 μ m^[51,52] and hy-

drophobic surface^[53,54] are favored for macrophage uptake, activation, and efficient immunity.^[55] We have used the diblock copolymer of PEG-*b*-PHMA, which offers balanced hydrophobic and hydrophilic properties. This copolymer type has been never reported in previous drug delivery systems that show lower diameter than our PMs (50–200 nm) and contain CSF1Ri to modulate macrophage repolarization response.^[38,39,56]

2.2. CSF1Ri-Loaded Polymersomes Are Macrophage Cytoprotective Compared to Free Drug

Blocking CSF1/CSF1R pathway has been shown to cause macrophage depletion through the induction of cell death.^[57] Different drug delivery approaches using $<10 \times 10^{-6}$ M BLZ945 have been proven to induce minimal toxicity to macrophages in in vivo models^[37–40,56] or in in vitro assays.^[40,56] Therefore the effect of CSF1Ri-loaded PMs on macrophage viability and cytotoxicity was assessed by both selective dye exclusion and lactate dehydrogenase (LDH) levels, respectively. Interestingly, CSF1Ri-loaded PMs induced less LDH-based macrophage cytotoxicity versus free drug upon 24 h ($p < 0.01$ vs $p < 0.001$) and 96 h ($p < 0.001$ vs $p < 0.0001$) incubation (**Figure 2**). Empty (e.g., nondrug loaded) PMs showed a minimum and nonsignificant cytotoxicity over 4 days. Further investigation in M2-like macrophages culture on-chip setting by selective dye exclusion confirmed that 48 h of 10×10^{-6} M of CSF1Ri-loaded PMs incubation preserved macrophage viability as untreated control. However, 10×10^{-6} M of free CSF1Ri reduced significantly macrophage viability versus untreated control (** $p < 0.01$) (**Figure S10**, Supporting Information). Together, these results suggest that CSF1Ri delivery by PMs causes less toxicity to macrophages compared to free drug.

2.3. CSF1Ri-Loaded Polymersomes Induce More Effective M2 to M1 Repolarization Compared to Free Drug

To examine the effect of CSF1Ri-loaded PMs on M2-like macrophage repolarization, we treated M2-like macrophages with free CSF1Ri, CSF1Ri-loaded PMs, and empty PMs during 48 h and monitored the effects on the expression levels of the M2 marker CD206⁺ and the M1 marker CD86⁺ by flow cytometry (**Figure 3a**). Treatment with CSF1Ri-loaded PMs resulted in the decrease of the CD206⁺/CD86⁺ marker expression ratio (e.g., M2 to M1 repolarization ratio) ($p < 0.05$) (**Figure 3b**). PMs and free CSF1Ri also reduced the M2 to M1 repolarization ratio in comparison to untreated control but the decrease was statistically nonsignificant ($p = 0.463$ and $p = 0.205$, respectively) (**Figure 3b**). Sustained inhibition of CSF1/CSF1R axis has been proposed to maintain macrophages in a continuous M1-like activated state for efficacious treatment against specific tumor types.^[58] This “mild or sustained repolarization” of M2 to M1-like macrophages, without completely depleting the available macrophage pool, seems to be better achieved by drug delivery systems based on the previously published studies.^[37–40,56] The lowest M2 to M1 repolarization ratios have been reported by using BLZ945 concentrations $> 500 \times 10^{-9}$ M in different combinatorial drug delivery systems.^[38,39] As shown in **Figure 3b**, CSF1Ri-loaded PMs significantly exhibited the lowest M2 to M1 repolarization ratio, which

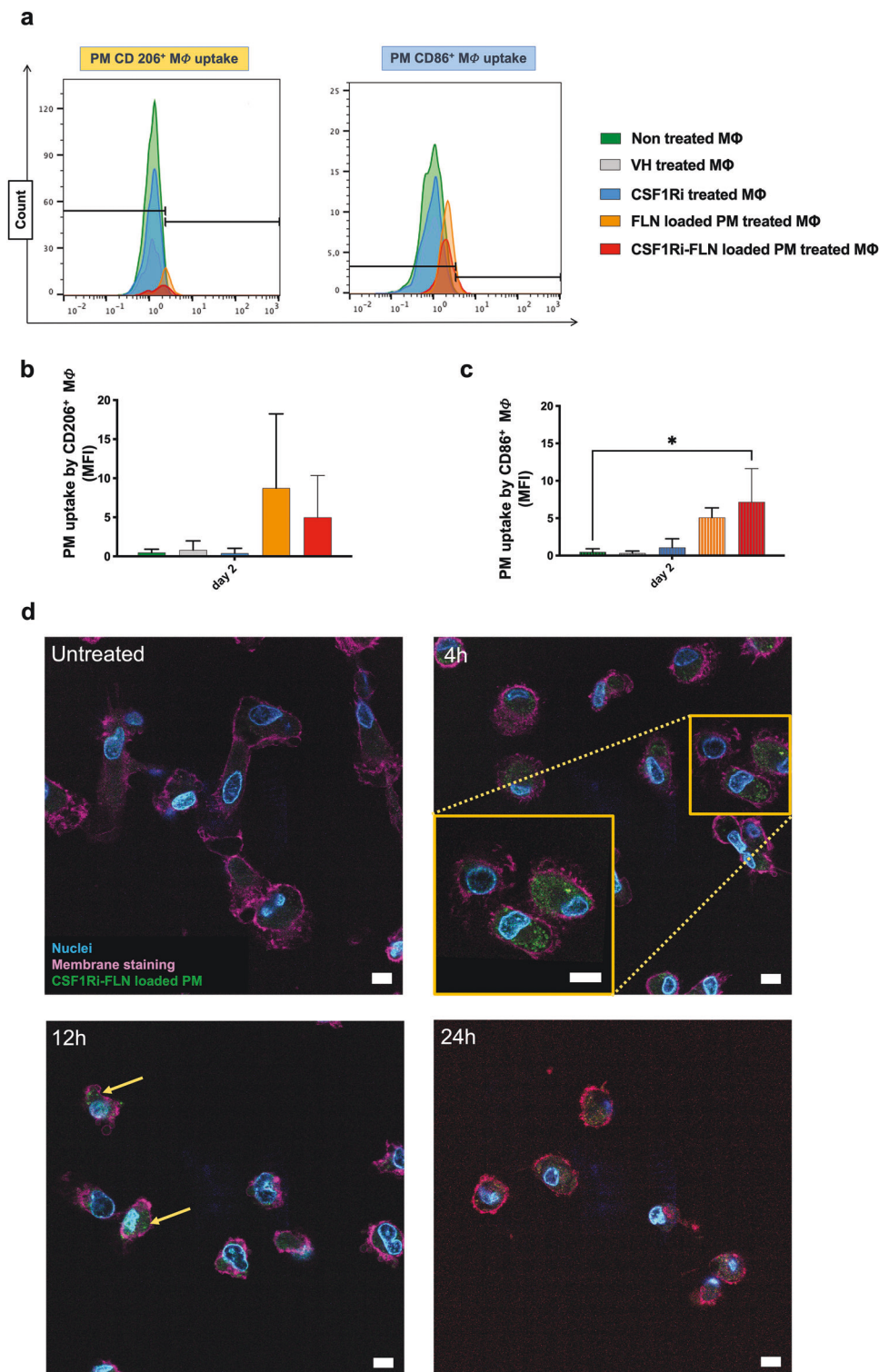


Figure 1. Uptake of fluorescein labeled PMs by M2-like macrophages (MΦ) assessed by flow cytometry and confocal microscopy. a) Fluorescence histograms of the flow cytometry analysis of nontreated macrophages and macrophages treated for 48 h with vehicle solution (VH), 10×10^{-6} M of free CSF1R inhibitor (CSF1Ri), fluorescein-loaded PMs (FLN-loaded PMs) and 8.5×10^{-6} M of CSF1Ri-FLN loaded PMs. M2-like macrophages: CD206⁺; M1-like macrophages: CD86⁺. b,c) Mean fluorescence intensity (MFI) quantification (e.g., uptake) of PMs-treated (b) CD11b⁺CD206⁺ and (c) CD11b⁺CD86⁺ macrophages. Statistical analysis was performed by one-way ANOVA followed by Dunnett's multiple comparisons. Results were considered significant with at least $p < 0.05$ (*) versus negative control. Results are expressed as mean + standard deviation ($n = 3$). d) Confocal microscopy images of M2-like macrophages incubated with CSF1Ri-loaded PMs. Arrows show presence of CSF1Ri-FLN loaded PMs within M2-like macrophages after 12 h incubation. Nuclei (blue), plasma membrane staining (magenta), and CSF1Ri-FLN loaded PMs (green). Scale bars: 10 μ m.

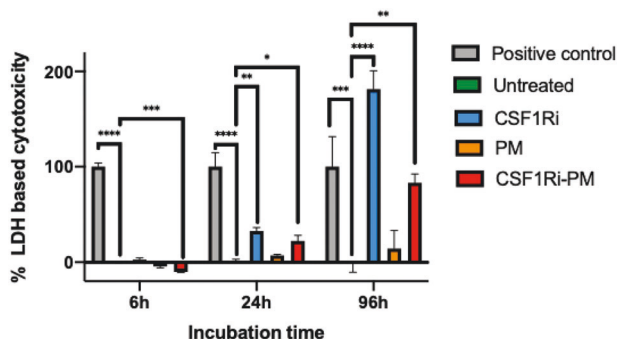


Figure 2. CSF1Ri-loaded PMs are macrophage cytoprotective compared to free drug. LDH release from M2-like macrophages upon CSF1Ri treatment for 6, 24, and 96 h is shown for the indicated treatments. Positive control (Triton-x, 0.1% v/v), untreated macrophages, 10×10^{-6} M of BLZ-945 drug (CSF1Ri), empty PMs and 10×10^{-6} M of CSF1Ri-PMs. LDH-based cytotoxicity in % was calculated as follows: $(\text{OD sample} - \text{OD negative control}) / (\text{OD positive control} - \text{OD negative control}) \times 100$. LDH data experiments were analyzed by a one-way ANOVA followed by Dunnett's multiple comparison. Results are expressed in triplicate ($N = 3$ technical replicates) as mean + standard deviation ($n = 1$). Results were considered statistically significant increased compared to untreated macrophages with at least $p < 0.01$ (*), $p < 0.001$ (**), $p < 0.0005$ (***), $p < 0.0001$ (****).

was 1.93-fold lower than untreated macrophages, whereas the vehicle (1:3 mixture of THF/H₂O v/v) and free CSF1Ri showed a 1.32–1.45 ratio. Particularly, macrophage survival depends on CSF1/CSF1R axis pathway signaling^[59] and macrophage treatment with BLZ945 (CSF1Ri) has been widely reported to reduce their viability.^[60] Propidium iodide (PI)-based-macrophage viability was constant across all conditions (untreated and treated cells), except in free CSF1Ri treatment with lower nonsignificant viability (Figure 3c). In comparison to PI-based cell viability marker from flow cytometry, live/dead cell viability assay showed higher sensitivity to detect significant differences as there is simultaneous fluorescent staining of both viable (intracellular esterase activity) and dead (plasma membrane integrity) cells (Figure S10b, Supporting Information). Expectedly, LDH levels assessment, a sensitive and definite endpoint, anticipated significant cytotoxicity differences of free drug compared to untreated control (Figure 2) in comparison to PI-based cell viability marker. Overall, these results indicate a sustained efficacy of the drug-loaded PMs on M2 to M1-like macrophage repolarization upon phagocytosis.

2.4. The M2 to M1-Like Macrophage Repolarization Induced by CSF1Ri-Loaded PMs Is Maintained in a Macrophage Coculture Model with MDA-MB-231 Breast Cancer Cells

CSF1R expression is widely distributed in the cells of myeloid lineage^[25] and tumor associated myeloid cells overexpress it for their own survival (e.g., acute myeloid leukemia or glioma).^[61,62] CSF1Ri treatments (alone or in combination) are currently being tested in clinical trials in patients with TNBC.^[63] As MDA-MB-231 express CSF1R protein (Figure S9, Supporting Information) and CSF1R mRNA,^[26] albeit at lower levels compared to M2-like macrophages,^[27] we also considered a possible direct cytotoxic effects of CSF1Ri on MDA-MB-231 cells. To test

this hypothesis, we treated MDA-MB-231 cells only with CSF1Ri and observed a low inhibitory effect on cell proliferation ($IC_{50} = 10.67 \times 10^{-3}$ M) (Figure S8, Supporting Information). M1-like macrophages have been proven to have direct and indirect tumoricidal mechanisms (release of proinflammatory cytokines) toward cancer cells.^[64] To examine the possible indirect tumoricidal effects of M2 to M1-like repolarized macrophages on TNBC cells, we first induced in vitro differentiation of pan macrophages to M2-like macrophages in the transwell inserts of a 2D coculture system containing the human MDA-MB-231 cells grown on the bottom of the well plate. Following macrophages differentiation, we treated M2-like macrophages with CSF1Ri for 5 days to induce M2 to M1-like repolarization and assessed macrophages viability using Crystal Violet staining (Figure 4a). As shown in Figure 4b, free CSF1Ri significantly depleted M2-like macrophages ($p < 0.01$) compared to the untreated control. By contrast, CSF1Ri-loaded PMs treatment effectively preserved macrophages viability (Mean + SD of $n = 2$: $87 \pm 19\%$ vs $63 \pm 11\%$, CSF1Ri-loaded PMs and free CSF1Ri, respectively), while retaining the effective M2 to M1 macrophage repolarization, as observed previously in single macrophage cell culture (Figure 3b). We next explored whether the increased presence of repolarized M1-like macrophages in cultures treated with CSF1Ri-loaded PMs may induce apoptosis or necrosis in MDA-MB-231 cells coculture for 5 days. As shown in Figure 4c, this longer survival of M2 to M1-like macrophages treated with CSF1Ri-loaded PMs did not have any significant impact on neither of the monocultures or cocultures MDA-MB-231 basal levels of apoptosis after 5 days. Indeed, we observed similar levels of late apoptosis and necrosis in monocultures either untreated or treated with vehicle, empty PMs, free and CSF1Ri-loaded PMs (upper panel, Figure 4c,d). These results are supported by the low inhibitory effect of CSF1Ri shown in this TNBC cell model (Figure S8, Supporting Information). A trend toward increased late apoptotic and necrotic cell populations was nevertheless observed in both free and CSF1Ri-loaded PMs treatment in 5 days cocultures. Coculture conditions late apoptosis: $p = 0.438$ and $p = 0.170$, free and CSF1Ri-loaded PMs versus negative control, respectively (lower panel, Figure 4d). Next, we tested CSF1Ri treatment during 7 days in a 3D macrophage-MDA-MB-231 coculture system, mimicking a more biologically relevant direct immune–cancer cell interaction. Flow cytometry analysis of treated cultures showed nonsignificant difference in apoptosis or necrosis of macrophage or MDA-MB-231 cells between the free or drug-loaded PMs and untreated control treatment (Figure S7b,c, Supporting Information).

Based on this data, flow cytometry analysis revealed that no apparent significant increased apoptotic or necrotic cell death occurred in either 2D monoculture, coculture system or 3D coculture system upon CSF1Ri treatment. Also, no major change in morphology was observed in the MDA-MB-231 cells upon CSF1Ri treatment independently of the 2D and 3D (Figure S7a, Supporting Information) coculture and timing conditions. These results indicate that repolarization of macrophages is not sufficient to trigger significant apoptosis in a TNBC coculture model.

3. Conclusion

The tumor immune environment plays a crucial role in modulating tumor growth and progression. Immunotherapy, given alone

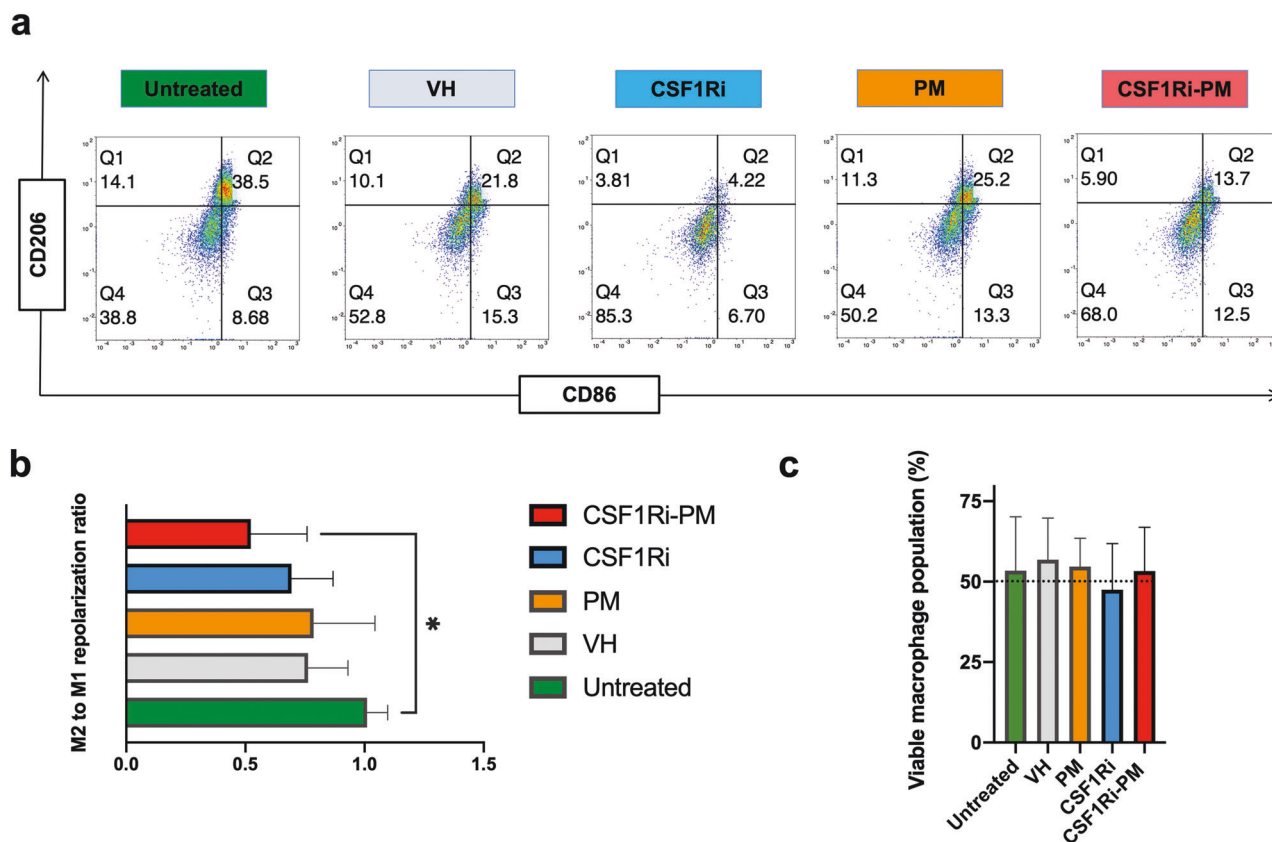


Figure 3. CSF1Ri-loaded PMs effectively repolarize M2-like macrophages toward M1-like macrophages. a) Representative flow cytometry plots showing CD11b⁺CD206⁺ (M2-like) and CD11b⁺CD86⁺ (M1-like) macrophages at 48 h of treatments: Untreated, vehicle solution (VH), 10×10^{-6} M of BLZ-945 drug (CSF1Ri), empty PMs, and CSF1Ri-PMs. b) M2 to M1 repolarization ratio. Quantification of flow cytometry plots showing ratio of expression of CD206 and CD86 on CD11b⁺ macrophages treated for 48 h post-M2 polarization. M2 to M1 repolarization ratio was calculated as division of Q1 (M2) + Q2 (M2 and M1)/Q3 (M1) + Q2 (M2 and M1) from each condition. Q1 represents M2-like macrophage positive for marker CD206. Q2 represents mixed M2 and M1-like macrophage positive for markers CD206 and CD86, respectively. Q3 represents M1-like macrophage positive for marker CD86. Q4 represents pan or naïve macrophages. c) Macrophage viability after CSF1Ri treatment. Results are given in percentage of negative propidium iodine (PI) stained and CD11b⁺ macrophage population. Statistical analysis was performed by one-way ANOVA followed by Dunnett's multiple comparisons. Results were considered significant with at least $p < 0.05$ (*) versus negative control. Results are expressed as mean + standard deviation ($n = 3$).

or in combination with other anticancer therapies, has become an emerging strategy for the treatment of cancer.^[65,66] Nevertheless, the clinical application of combinatorial cancer immunotherapies remains a challenge in most of tumor types due to limited efficacy and safety profile.^[67] Future cancer immunotherapy needs to become safer and more efficacious by reducing off-target toxicities while improving antitumor activity. To this end, many delivery strategies have been developed and tested preclinically, and a few clinical studies have been performed and reported.^[68,69] These strategies aim to improve targeted delivery and local accumulation of immunotherapy drugs by selectively targeting tumor cells directly or educating immune cells in the tumor target environment. For example, targeting cells with spatially constrained 2-in-1 nanomedicine delivery systems has been proved to enhance efficacy compared to single drug payload stochastic distribution.^[70] Despite of promising drug delivery nanocarriers that modulate tumoral immune response,^[71] these novel approaches still bear some limitations, such as premature drug release, delivery to off-target clearance organs, nanocarrier instability or systemic toxicity.^[69]

In this study we addressed the question of repolarizing tumor associated macrophages toward a more tumoricidal phenotype in safer manner by developing and testing the uptake of CSF1Ri-loaded PMs, evaluating their toxicity and comparing the effect of free versus PMs encapsulated CSF1Ri on M2- to M1-like macrophage repolarization and survival of cocultured breast cancer cell in vitro model. We show that CSF1Ri-loaded PMs induce an effective M2 to M1-like macrophage repolarization in vitro while preserving macrophage viability. Albeit there were no immediate effects on MDA-MB-231 cell viability reduction in 2D transwell and 3D direct coculture models, CSF1Ri loaded PMs could maintain macrophage viability and an apparent M2 to M1-like macrophage repolarization. Remarkably, CSF1Ri encapsulation by PEG-*b*-PHMA copolymer PMs has shown to modulate a sustained repolarization response of TAMs.

Overall, this finding supports the notion that improved drug targeting of tumor associated macrophages, can significantly contribute to enhance the M2 to M1-like macrophage repolarization effect with potential therapeutic benefits. This versatile approach represents a promising tool that may be applied to

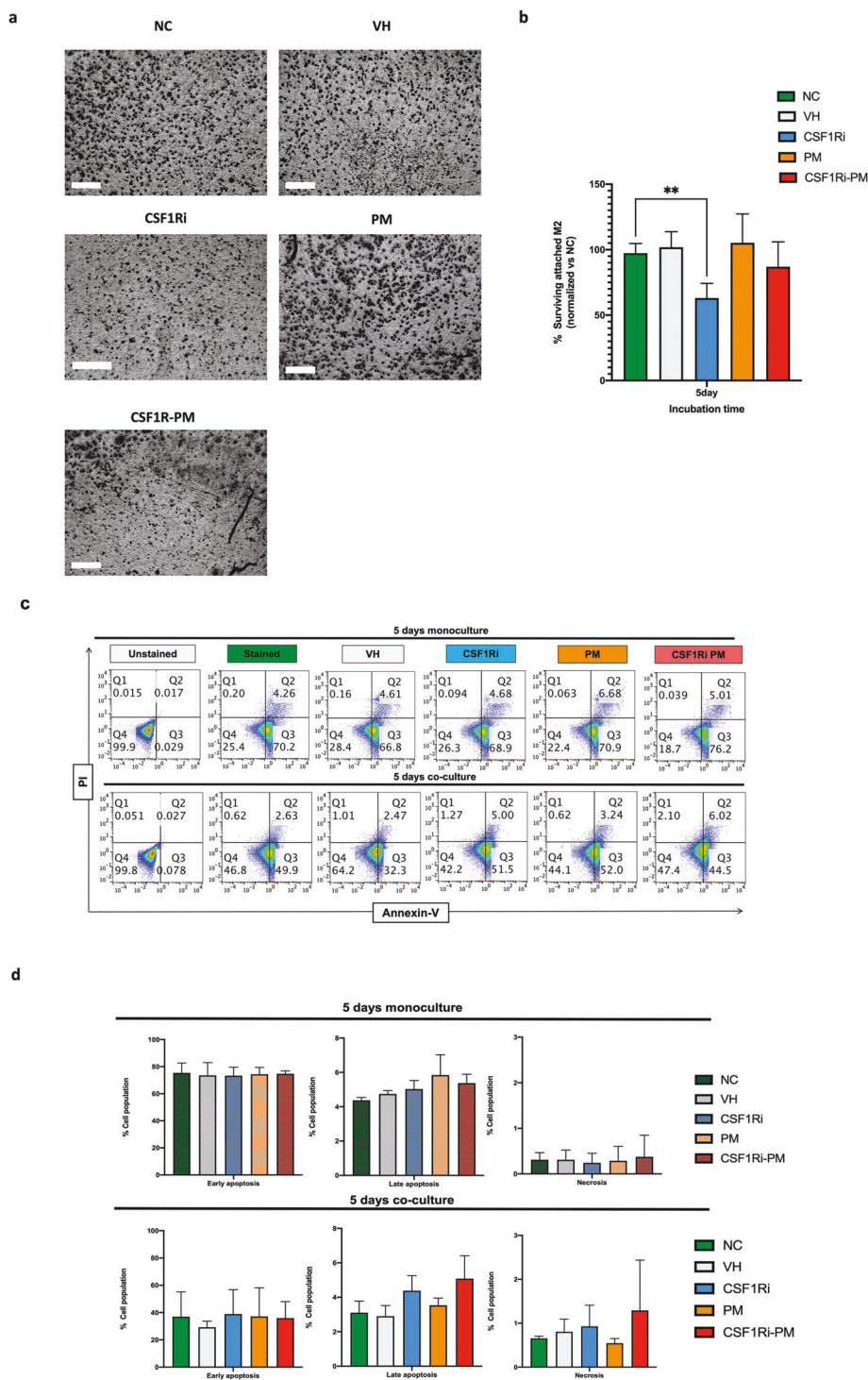


Figure 4. CSF1Ri treatment of a macrophages-MDA-MB-231 transwell coculture system. a) Images of M2-like macrophages cocultured with MDA-MB-231 in a transwell system after 5 days of CSF1Ri treatment. Macrophages were stained with Crystal Violet (CV) and photographed with EVOS M5000 imaging system. Scale bars: 400 μ m. b) Relative quantification of M2-like macrophages viability. Quantification was performed by colorimetric determination of CV staining. Statistical analysis was performed by a one-way ANOVA followed by Dunnett's multiple comparisons. Results were normalized and considered significant with at least $p < 0.01$ (**) versus negative control. Results expressed as mean + standard deviation ($n = 2$). c) Representative flow cytometry analysis of Annexin V/propidium iodide-based apoptosis/necrosis assay in MDA-MB-231 cells upon monoculture or coculture with M2-like macrophages in transwell after 5 days of CSF1Ri treatment. Top panel: MDA-MB-231 monoculture. Bottom panel: M2-like macrophages-MDA-MB-231 coculture. Negative control (NC), unstained, vehicle solution (VH), 10×10^{-6} M of BLZ-945 drug (CSF1Ri), empty PMs, and CSF1Ri-PMs. d) Quantification of apoptotic/necrotic cells. Analysis shows early and late apoptotic and necrotic MDA-MB-231 cells upon indirect coculture of CSF1Ri treated M2-like macrophages. Results expressed as mean + standard deviation ($n = 2$).

enhance the activity of currently and future immunotherapy strategies.

4. Experimental Section

Materials: 1-Ethyl-3-(3-dimethylaminopropyl)carbodiimide, 2 kDa poly(ethylene glycol) monomethyl ether, 4-cyano-4-(phenylcarbonothioylthio) pentanoic acid, azobisisobutyronitrile, hexyl methacrylate, fluorescein disodium salt, 4-dimethylaminopyridine, and 1,4-dioxane were purchased from Sigma-Aldrich. Dichloromethane (CH_2Cl_2) and tert-butyl methyl ether were purchased from Reactolab SA. Deuterated chloroform was purchased from Apollo Scientific. Methanol and THF were purchased from Fisher Scientific.

Size Exclusion Chromatography (SEC): SEC experiments were performed on an Agilent 1200 series HPLC system equipped with an Agilent PLgel mixed guard column (particle size = 5 μm) and two Agilent PLgel mixed-D columns (ID = 7.5 mm, L = 300 mm, particle size = 5 μm). Signals were recorded by a UV detector (Agilent 1200 series), an Optilab REX interferometric refractometer, and a miniDawn TREOS light scattering detector (Wyatt Technology Corp.). Samples were run using THF as the eluent at 30 °C and a flow rate of 1.0 mL min^{-1} . Data analyses were carried out on Astra software (Wyatt Technology Corp.) and molecular weights were determined based on narrow molecular weight polystyrene standards calibration (from 540 to 2 210 000 g mol^{-1}).

NMR Spectroscopy: NMR spectra were recorded on a Bruker Avance III 300 MHz NMR spectrometer (^1H NMR 300 MHz, ^{13}C NMR 75 MHz) or a Bruker Avance III 400 MHz NMR spectrometer (^1H NMR 400 MHz, ^{13}C NMR 101 MHz).

Dynamic Light Scattering (DLS): DLS data were obtained with 2 mL of a dilute aqueous dispersion of the PMs. Data were collected at constant temperature (25 °C) on a commercial goniometer instrument (3D LS Spectrometer, LS Instruments AG, Switzerland) at angle 90°. The primary beam was formed by a linearly polarized and collimated laser beam (Cobolt 05-01 diode pumped solid state laser, $\lambda = 660$ nm, $P_{\text{max}} = 500$ mW), and the scattered light was collected by single-mode optical fibers equipped with integrated collimation optics. The incoming laser beam passed through a Glan–Thompson polarizer with an extinction ratio of 10^{-6} . Another Glan–Thompson polarizer, with an extinction ratio of 10^{-8} , was mounted in front of the collection optics. To construct the intensity autocorrelation function $g_2(t)$, the collected light was coupled into two APD detectors via laser-line filters (Perkin Elmer, Single Photon Counting Module), and their outputs were fed into a two-channel multiple-tau correlator. To improve the signal-to-noise ratio and to eliminate the impact of detector after-pulsing on $g_2(t)$ at early lag times below 1 μs , these two channels were cross-correlated. The field autocorrelation function was obtained via the Siegert relation: $g_1(t) = \sqrt{g_2(t) - 1}$. The hydrodynamic radius (R_h) was determined from the Stokes–Einstein relation

$$R_h = \frac{k_B T}{6\pi\eta D} \quad (1)$$

where k_B is the Boltzmann constant, T the temperature, η the viscosity of the solvent, and D the diffusion coefficient was determined using a second order cumulant fit of $g_2(t)$.

Synthesis of the Block Copolymer: The diblock copolymer was synthesized following a procedure inspired from the literature.^[72] Briefly, a poly(ethylene glycol) 4-cyano-4-(phenylcarbonothioylthio) pentanoate chain transfer agent (CTA) was first synthesized by 1-ethyl-3-(3-dimethylaminopropyl)carbodiimide EDCI coupling of monomethyl poly(ethylene glycol) (PEG) and 4-cyano-4-(phenylcarbonothioylthio) pentanoic acid. In a 20 mL vial, EDCI (555 mg, 2.89 mmol) was dissolved in 6 mL CH_2Cl_2 . In a 25 mL round-bottom flask, poly(ethylene glycol) monomethyl ether 2 kDa (2.40 g, 1.20 mmol), 4-cyano-4-(phenylcarbonothioylthio) pentanoic acid (822 mg, 2.94 mmol), and DMAP (38.1 mg, 0.300 mmol) were dissolved in 12 mL CH_2Cl_2 . Both solutions were introduced in a freezer at -20 °C for 1 h. Then, the EDCI suspension was added drop-by-drop to the second solution. The resulting mixture

was let to warm up to room temperature (RT) and was stirred for 48 h. The solution was precipitated in cold (0 °C) tert-butyl methyl ether and dissolved again in CH_2Cl_2 . The process was repeated three times to yield a pure functionalized polymer. The resulting diblock copolymer (PEG-CTA, $M_n = 2.2$ kDa, $\mathcal{D} = 1.04$) was purified and characterized (Figures S1 and S2, Supporting Information) as described in the literature.^[72] Then, the CTA was chain-extended with hexyl methacrylate (HMA) by reversible addition–fragmentation chain-transfer polymerization: AIBN (3.0 mg, 18.3 μmol) and the PEG-CTA (292 mg, 148 μmol) were dissolved in 2.3 mL of 1,4-dioxane. The monomer HMA was purified by filtering it through a basic aluminum oxide plug. Then, purified HMA (1.24 mL, 8.2 mmol) was added to the AIBN and PEG-CTA solution. The mixture was bubbled for 1 h with argon then, heated at 90 °C under argon for 2 h before exposing the solution to the atmosphere. The polymer was precipitated in a cold (0 °C) 6:4 methanol/water mixture. The resulting diblock copolymer (PEG-*b*-PHMA, $M_n = 13$ kDa, $\mathcal{D} = 1.15$) was purified and characterized (Figures S1 and S2, Supporting Information) as described in the literature.^[72]

Self-Assembly of Block Copolymers into PMs: The PMs suspensions were synthesized following a procedure inspired from the literature.^[49] In a 20 mL vial, the PEG-*b*-PHMA copolymer (1.5 mg) was dissolved in THF (1 mL) and PBS pH = 7.4 aqueous buffer (10 mL) was added dropwise over 10 min. The suspension was filtered at RT over 0.8 and 0.4 μm track-etch membrane using an Avanti Polar Lipids extruder before dialysis (regenerated cellulose membrane, 1 kDa molecular weight cut off in PBS buffer over 5 days (1 L changed ten times)). For the CSF1Ri-loaded particles, the drug (10 mg) was added to the organic solvent at a concentration of 25×10^{-3} M while for the fluorescein (376.27 g mol^{-1} , FLN) loaded particles, the dye (25 mg) was added to the 10 mL aqueous buffer at a concentration of 7×10^{-3} M. The PMs were characterized by LS (Table S1, Supporting Information) where the ratio of the gyration radius (R_g) measured by static light scattering (SLS) and the hydrodynamic radius (R_h) measured by DLS of all the PMs suspensions were close to 1.0, which indicates a vesicle morphology, i.e., polymersomes.^[64]

The final concentration of CSF1Ri (c_{CSF1Ri}) was measured by UV/vis spectroscopy (Table S2, Supporting Information): an aliquot (0.4 mL) of the PMs suspension was dissolved in chromatographic THF (1.6 mL) and the absorbance of the resulting solution was measured from 250 to 700 nm (Figure S3, Supporting Information). The copolymer, FLN, and CSF1Ri concentrations were determined via linear calibration curves for each analyte. The concentration of copolymer was assumed to be similar in all the suspension. In the CSF1Ri–FLN suspension, the concentration of FLN was first determined with the $\lambda = 485$ nm signal before removing the contribution of copolymer and FLN dye from the main signal. The calibrations were achieved by measuring the analyte absorbance signal at different concentration (Figure S4, Supporting Information).

CSF1 Inhibitor Preparation for In Vitro Studies: BLZ-945 (A15540-50, Hölzel Diagnostika) (0.001g, 2.5×10^{-3} M) was dissolved from a stock in vehicle solution or VH (1 mL of 1:3 mixture of THF/ H_2O v/v) and sonicated in a water bath at 50 °C for 15 min. This drug concentration was further diluted in VH to the desired working concentration.

Cell Cultures: MDA-MB-231 cells were cultured in complete RPMI-1640 or cRPMI (21875-034, Gibco, LifeTechnologies) supplemented with 10% fetal bovine serum (FBS) (P40-37500, PAN-Biotech, Germany) and 1% penicillin/streptomycin (10000 U mL^{-1} , 15140122, ThermoFisher). Culture medium was changed every 3–4 days, passaged at $\approx 80\%$ confluency using 0.05% Trypsin-EDTA (15400-045, Gibco, LifeTechnologies). Absence of mycoplasma contamination from MDA-MB-231 during the experiments was confirmed by using the PCR mycoplasma Test Kit I/C (PromoCell).

Primary Human Monocyte-Derived Macrophages (MDMs) Isolation and M2-Like Phenotype Differentiation: Monocyte Isolation: Work involving primary human MDMs was approved by the Federal Office for Public Health Switzerland (reference number: 611-1, Meldung A110635/2). Macrophages were prepared from whole buffy coat following a previously developed protocol.^[73] Peripheral blood mononuclear cells were isolated from buffy coats provided by the Swiss Transfusion Centre (Bern, Switzerland). Magnetic beads (Milteny Biotec GmbH, Germany) were used to select for CD14⁺ monocytes.

Monocyte-Macrophage Differentiation: For MDMs differentiation, monocytes were cultured at a density of 1×10^6 cells per well during 3 days in 6-well tissue culture plates (3516, Corning) with macrophage supplemented culture medium. Then, pan macrophages were harvested by using Accutase (A6964, Sigma) and differentiated with M2-like macrophage culture medium (sM2) during 2 days on coverslips or cell well plates for imaging or flow-cytometry experiments, respectively. Macrophage supplemented culture medium contained Gibco RPMI supplemented with 15% FBS (P40-37500, PAN-Biotech, Germany), 1% penicillin–streptomycin ($10\,000\text{ U mL}^{-1}$, 15140122, ThermoFisher), 0.01% L-glutamine 1 \times (25030-024, ThermoFisher), and 10 ng mL^{-1} M-CSF1 (PHC9504, ThermoFisher). For sM2 medium preparation, 20 ng mL^{-1} IL-4 (200-04, PeproTech), IL-10 (200-10, PeproTech), and IL-13 (200-13, PeproTech) were added to macrophage supplemented culture medium.

M2-Like Macrophage Repolarization and Uptake of PMs Using Flow Cytometry: Pan macrophages were cultured at 8×10^4 cells per well in 12-well-plate (07-201-589, Corning) and differentiated with 1 mL sM2 during 2 days. 12-well-plate were previously pretreated with poly-D-lysine (P4707-50ML, ThermoFisher) for 20 min on the incubator at 37°C , 5% CO_2 and 1 \times PBS washed before seeding macrophages. Then, drug treatment of M2-like macrophages repolarization followed during 2 days within 0.5 mL volume per well. The summary of the drug treatments is presented in Table 1.

After drug treatment, nonadherent and adherent macrophages were collected by using Accutase (A6964, Sigma), gently washed with cold running buffer (1% BSA, Running Buffer MACSQuant, 130-092-747, Miltenyi Biotec) and centrifuged (500 RCF, 5 min at 4°C).

Macrophages were stained with the following flow cytometry antibodies at the concentrations recommended by the manufacturer: anti-CD11b-PE-Cy7 (clone ICRF44; 557743 BD), anti-CD86-PE (clone BU63, 374205, BioLegend), anti-CD206-FITC (clone 15.2, 321103, BioLegend), as human pan macrophages, M1 macrophage, and M2 macrophage markers, respectively, in cold running buffer containing PI (BMS500PI, ThermoFisher) for dead cell exclusion. Additional untreated samples were prepared for fluorescence minus one control staining using OneComp eBeads compensation beads (01-1111-41, Thermo Fisher Scientific) to set up the cytometer. After antibody labeling for 20 min at 4°C in the dark, cells were centrifuged (500 RCF, 5 min, 4°C) and gently washed in 1 \times cold running buffer and stored at 4°C before data acquisition. Data were acquired using MACSQuant Analyzer 10 flow cytometer (Miltenyi Biotec, Bergisch Gladbach, Germany) and analyzed using FlowJo Software (v10.6.2, FlowJo LLC).

Monoculture and Indirect Cocultures of MDA-MB-231 and Macrophages (Transwell Assay): For MDA-MB-231 monocultures, 5×10^4 cells per well were cultured on 24-well plate (353504, Corning) for 1 day in 0.5 mL complete RPMI medium. For the indirect cocultures, MDA-MB-231 were cultured at 5×10^4 cells per well on 24-well plate (353504, Corning) for 1 day in 0.5 mL complete RPMI medium before merging them into the indirect coculture with M2-like macrophages. Pan macrophages were cultured at 25×10^3 cells per insert in 24-well-inserts (PET, pore size: $0.4\ \mu\text{m}$; 353095, BD Falcon) and differentiated with 0.5 mL of macrophage stimulation cell culture medium (sM2) during 2 days. Bottom wells were covered with 0.5 mL of sM2. Transwell inserts were previously pretreated with poly-D-lysine (P4707-50ML, ThermoFisher) for 20 min on the incubator at 37°C , 5% CO_2 , and 1 \times PBS washed before seeding macrophages. After 2 days of M2 phenotype stimulation, fresh 0.25 mL sM2 was added to the inserts (top) before coculture of them with MDA-MB-231 wells in 0.5 mL cRPMI (bottom). A physical contact between membrane insert and cell culture medium from bottom well was secured. Drug treatments in cRPMI (for monocultures) or sM2 (for indirect coculture) were added and cells were incubated at 37°C , 5% CO_2 during 5 days. The summary of the treatments is presented in Table 2.

MDA-MB-231 Cancer Apoptosis Assay: Adherent and MDA-MB-231 cells in suspension were collected from the 24-well plate using 1 \times Trypsin (15400-054, ThermoFisher) and incubated in 100 μL of binding buffer ($50 \times 10^{-3}\text{ M}$ (4-(2-hydroxyethyl)-1-piperazineethanesulfonic acid) or HEPES ($700 \times 10^{-3}\text{ M}$ NaCl, $12.5 \times 10^{-3}\text{ M}$ CaCl_2 , pH 7.4) containing 3 μL of Annexin V-PE (640941, BioLegend) during 20 min at RT, protected from light. 5 min before analysis by flow cytometry, 1 μL of $100\ \mu\text{g mL}^{-1}$

PI (BMS500PI, ThermoFisher) was added to the cell suspension. Then, 200 μL of 1 \times Annexin-binding buffer was added to the cell suspension and mixed gently. Data were acquired using MACSQuant Analyzer 10 flow cytometer (Miltenyi Biotec, Bergisch Gladbach, Germany) and analyzed using FlowJo Software (v10.6.2, FlowJo LLC).

Crystal Violet Staining and Quantification: Transwell inserts were previously pretreated with poly-D-lysine (P4707, ThermoFisher) before macrophage seeding. After macrophage treatment, the macrophages-bearing inserts (PET, pore size: $0.4\ \mu\text{m}$; 353095, BD Falcon) were washed with 1 \times PBS. Then macrophages were gently fixed with 4% formaldehyde (818708, Sigma) by putting 50 μL per insert and 400 μL into the P24 bottom well for 15 min at RT. Staining followed by adding 200 μL of crystal violet (C0121, Beyotime) for 1 h. Then transwell inserts were washed with 1 \times PBS to remove unbound crystal violet and then air-dried for 2 h. The fixed macrophages from inserts were imaged with EVOS M5000 imaging system (ThermoFisher) before crystal violet quantification. The bound crystal violet was eluted by adding 400 μL of 33% acetic acid (10000208, Sinopharm) into each insert and shaking for 10 min. The eluent within the insert was transferred in triplicates to a 96 well clear microplate (3599, Corning) and the absorbance was measured at 590 nm using a plate reader Tecan infinite M200 Pro.

LDH Release Assay: Macrophage cytotoxicity by CSF1Ri was evaluated by LDH (cytosolic enzyme) released in sM2 cell culture medium, analyzed in triplicate using LDH cytotoxicity detection kit (Roche Applied Science, Mannheim, Germany) according to the manufacturer's protocol. The absorbance of the colorimetric product was determined spectrophotometrically (Benchmark Microplate reader, BioRad, Switzerland) at 490 nm with a reference wavelength of 630 nm with 5 min intervals for three measurements.

MDA-MB-231 and Macrophages Aggregates Formation and Apoptosis Assay: For MDMs differentiation, monocytes were cultured at a density of 1×10^6 cells during 3 days in 6-well tissue culture plates (3516, Corning) with macrophage supplemented culture medium. Then, pan macrophages were harvested by using Accutase (A6964, Sigma) and used for the aggregate coculture. M2-like macrophages and MDA-MB-231 aggregates were formed under nonadhesive conditions by seeding 5×10^3 macrophages and 10×10^3 cells and (ratio 1:2), respectively, into ultralow attachment U-bottom 96-well plates (174925, Nunclon TM). A cRPMI and sM2 culture medium 50:50 v/v was used for the aggregate growth. Aggregates were treated with (a) complete RPMI medium (negative control), (b) vehicle or VH (1:3 mixture of THF/H₂O v/v), (c) $10 \times 10^{-6}\text{ M}$ of free drug (CSF1Ri), (d) empty PMs, and (e) CSF1Ri-loaded PMs for 7 days prior to the flow-cytometry assay. MDA-MB-231 cell and M2-like macrophages aggregates were collected, 1 \times PBS washed and incubated in 100 μL of binding buffer ($50 \times 10^{-3}\text{ M}$ HEPES, $700 \times 10^{-3}\text{ M}$ NaCl, $12.5 \times 10^{-3}\text{ M}$ CaCl_2 , pH 7.4) containing 3 μL of anti-CD11b-PE-Cy7 (clone ICRF44; 557743 BD) and 3 μL of Annexin V-PE (640941, BioLegend) during 20 min at RT, protected from light. 5 min before analysis by flow cytometry, 1 μL of $100\ \mu\text{g mL}^{-1}$ PI (BMS500PI, ThermoFisher) was added to the cell suspension. Then, 200 μL of 1 \times Annexin-binding buffer was added to the cell suspension and mixed gently. Data were acquired using MACSQuant Analyzer 10 flow cytometer (Miltenyi Biotec, Bergisch Gladbach, Germany) and analyzed using FlowJo Software (v10.6.2, FlowJo LLC).

Confocal Microscopy: Pan macrophages were cultured in 35 mm Dish, No. 1.5 Coverslip (P35G-1.5-14-C, Mtek) at 1×10^5 cells and treated with sM2 during 2 days. Coverslips were previously pretreated with poly-D-lysine (P4707-50ML, ThermoFisher) during 20 min in incubator at 37°C , 5% CO_2 . Then, macrophages were treated with CSF1Ri–FLN PMs for 4, 12, and 24 h. At the predetermined time points, macrophages were three times \times PBS washed and fixed with 4% para-formaldehyde (47608, Sigma). Attached macrophages were stained with $1\ \mu\text{g mL}^{-1}$ cytoplasm membrane staining-Alexa Fluor 680 (W32465, Thermo Fisher Scientific) and $1\ \mu\text{g mL}^{-1}$ Hoechst 33342 (H3570, Thermo Fisher Scientific) during 1 h. Confocal imaging was performed on a Leica TCS SP5 inverted microscope (Leica Microsystems GmbH, Mannheim, Germany) using a Plan-Apochromat 63 \times /1.30 NA oil objective (Zeiss GmbH, Jena, Germany). Laser lines 405, 488, and 633 nm were used for Hoechst 33452, FLN and cytoplasm membrane staining-Alexa Fluor 680 excitation, respectively. Af-

ter acquisition, PMs internalization analysis was performed using the fluorescent intensity profile function of ZEN software (ZEN, version 3.3, blue edition; Zeiss GmbH, Jena, Germany).

MTT Cell Viability Assay: MDA-MB-231 cells were seeded in 96-well plates with a density of 5×10^3 cells per well and preincubated overnight in cRPMI medium. The next day, the medium was aspirated, and cells were treated with free CSF1Ri at tenfold different concentrations (0.001×10^{-9} M, 0.01×10^{-9} M, 0.1×10^{-9} M, 1×10^{-9} M, 10×10^{-9} M, 100×10^{-9} M, 1×10^{-6} M, and 100×10^{-6} M) in cRPMI medium for 48 h. Then, the medium was discarded, and cells were incubated in 100 μ L of fresh medium containing 0.5 mg mL⁻¹ 3-(4,5-dimethylthiazol-2-yl)-2,5-diphenyl tetrazolium bromide (MTT, M2003, Sigma-Aldrich) for 2 h. After incubation, the medium was discarded again, the MTT formazan product was solubilized with 400 μ L dimethyl sulfoxide. The absorbance was measured at 570 nm with a spectrophotometer (TECAN infinite M200PRO, Männedorf, Switzerland).

Cell Viability of Macrophages Culture On-Chip: Cell viability was performed following manufacture's instructions (LIVE/DEAD assay, R37601, Thermo Fisher). MDMs were differentiated into M2-like macrophages in two steps: 1) in P6 well plate (833335, Corning) during 3 days in macrophage supplemented culture medium; 2) 40×10^3 pan macrophages were cultured in the lateral chamber from channel interaction chip (10001347, ChipShop GmbH) during 2 days in sM2. Then 5 days of treatment followed: untreated, 10×10^{-6} M of BLZ945 (CSF1Ri) and 10×10^{-6} M of CSF1Ri-PMs. Chip chambers were previously coated with poly-D-lysine (P4707-50ML, ThermoFisher) for 20 min on the incubator at 37 °C, 5% CO₂. Reagents (LIVE/DEAD assay, R37601, Thermo Fisher) were added to each chamber in PBS and incubated for 30 min prior to imaging with an M5000 EVOS microscope, ThermoFisher. Cell viability was determined by counting the number of live and dead stained cells from two representative areas selected at random for three biologically independent replicates. Viability was determined using the following equation

$$x = \frac{\text{live}}{\text{live} + \text{dead}} \times 100 \quad (2)$$

Statistical Analysis: Data experiments were analyzed by a one-way ANOVA followed by Dunnett's multiple comparison. All statistical analyses were performed with GraphPad Prism version 9.0.2 software (La Jolla, CA, USA). Only statistically significant differences ($p < 0.05$) are indicated in the figures.

Supporting Information

Supporting Information is available from the Wiley Online Library or from the author.

Acknowledgements

This research was supported by the Swiss National Science Foundation through the National Centre of Competence in Research (NCCR) Bio-Inspired Materials (Grant No. 51NF40-182881) and through Grant No. 310030L182725/1, as well as by the Medic foundation. The authors also acknowledge the Adolphe Merkle Foundation. The authors thank Sarah Cattin and Grégory Bieler for their technical support.

Open access funding provided by Université de Fribourg.

Conflict of Interest

The authors declare no conflict of interest.

Data Availability Statement

The data that support the findings of this study are openly available in ZENODO at <https://doi.org/10.5281/zenodo.5895076>, reference number 22032022.

Keywords

block copolymer vesicles, drug delivery systems, immunotherapies, polymersomes, triple negative breast cancer, tumor associated macrophages

Received: April 28, 2022

Published online: June 21, 2022

- [1] E. Nasrollahzadeh, S. Razi, M. Keshavarz-Fathi, M. Mazzone, N. Rezaei, *Cancer Immunol. Immunother.* **2020**, *69*, 1673.
- [2] H. Gonzalez, I. Robles, Z. Werb, *FEBS J.* **2018**, *285*, 654.
- [3] V. Riabov, A. Gudima, N. Wang, A. Mickley, A. Orekhov, J. Kzhyskowska, *Front Physiol* **2014**, *5*, 75.
- [4] G. Solinas, G. Germano, A. Mantovani, P. Allavena, *J Leukoc Biol* **2009**, *86*, 1065.
- [5] S. Vinogradov, G. Warren, X. Wei, *Nanomedicine (London, England)* **2014**, *9*, 695.
- [6] T. Chanmee, P. Ontong, K. Konno, N. Itano, *Cancers (Basel)* **2014**, *6*, 1670.
- [7] B. Z. Qian, J. W. Pollard, *Cell* **2010**, *141*, 39.
- [8] M. Herrera, A. Herrera, G. Domínguez, J. Silva, V. García, J. M. García, I. Gómez, B. Soldevilla, C. Muñoz, M. Provencio, Y. Campos-Martin, A. García de Herrerros, I. Casal, F. Bonilla, C. Peña, *Cancer Sci.* **2013**, *104*, 437.
- [9] Y. Komohara, Y. Fujiwara, K. Ohnishi, M. Takeya, *Adv Drug Deliv Rev* **2016**, *99*, 180.
- [10] K. Sawa-Wejksza, M. Kandefer-Szerszeń, *Arch Immunol Ther Exp (Warsz)* **2018**, *66*, 97.
- [11] M. Locati, G. Curtale, A. Mantovani, *Annu Rev Pathol* **2020**, *15*, 123.
- [12] A. Sica, A. Mantovani, *J. Clin. Invest.* **2012**, *122*, 787.
- [13] F. Balkwill, A. Mantovani, *Lancet* **2001**, *357*, 539.
- [14] F. Balkwill, K. A. Charles, A. Mantovani, *Cancer Cell* **2005**, *7*, 211.
- [15] L. M. Coussens, Z. Werb, *Nature* **2002**, *420*, 860.
- [16] A. Mantovani, T. Schioppa, C. Porta, P. Allavena, A. Sica, *Cancer Metastasis Rev.* **2006**, *25*, 315.
- [17] C. E. Lewis, J. W. Pollard, *Cancer Res.* **2006**, *66*, 605.
- [18] S. K. Biswas, P. Allavena, A. Mantovani, *Semin Immunopathol* **2013**, *35*, 585.
- [19] L. Q. Fu, W. L. Du, M. H. Cai, J. Y. Yao, Y. Y. Zhao, X. Z. Mou, *Cell. Immunol.* **2020**, *353*, 104119.
- [20] L. Cassetta, J. W. Pollard, *Nat. Rev. Drug Discovery* **2018**, *17*, 887.
- [21] Y. Shu, P. Cheng, *Biochim Biophys Acta Rev Cancer* **2020**, *1874*, 188434.
- [22] M. Molgora, M. Colonna, *Med (N Y)* **2021**, *2*, 666.
- [23] D. Achkova, J. Maher, *Biochem. Soc. Trans.* **2016**, *44*, 333.
- [24] A. R. Sullivan, F. J. Pixley, *J Mammary Gland Biol Neoplasia* **2014**, *19*, 149.
- [25] E. R. Stanley, V. Chitu, *Cold Spring Harb Perspect Biol* **2014**, *6*, 021857.
- [26] A. Morandi, V. Barbetti, M. Rivero, P. Dello Sbarba, E. Rovida, *PLoS One* **2011**, *6*, 27450.
- [27] C. V. Jones, S. D. Ricardo, *Organogenesis* **2013**, *9*, 249.
- [28] M. A. Cannarile, M. Weisser, W. Jacob, A.-M. Jegg, C. H. Ries, D. Rüttinger, *J. Imm. Ther. Cancer* **2017**, *5*, 53.
- [29] M. T. Saung, S. Muth, D. Ding, D. L. Thomas, 2nd, A. B. Blair, T. Tsujikawa, L. Coussens, E. M. Jaffee, L. Zheng, *J Immunother Cancer* **2018**, *6*, 118.
- [30] Q. Xun, Z. Wang, X. Hu, K. Ding, X. Lu, *Curr. Med. Chem.* **2020**, *27*, 3944.
- [31] D. A. Hume, K. P. MacDonald, *Blood* **2012**, *119*, 1810.
- [32] W. A. Denny, J. U. Flanagan, *Expert Opin. Ther. Pat.* **2021**, *31*, 107.
- [33] F. Peyraud, S. Cousin, A. Italiano, *Curr. Oncol. Rep.* **2017**, *19*, 70.
- [34] W. D. Tap, H. Gelderblom, E. Palmerini, J. Desai, S. Bauer, J. Y. Blay, T. Alcindor, K. Ganjoo, J. Martín-Broto, C. W. Ryan, D. M. Thomas, C.

- Peterfy, J. H. Healey, M. van de Sande, H. L. Gelhorn, D. E. Shuster, Q. Wang, A. Yver, H. H. Hsu, P. S. Lin, S. Tong-Starksen, S. Stacchiotti, A. J. Wagner, *Lancet* **2019**, 394, 478.
- [35] F. Lei, N. Cui, C. Zhou, J. Chodosh, D. G. Vavvas, E. I. Paschalis, *Proc. Natl. Acad. Sci. USA* **2020**, 117, 23336.
- [36] T. A. Muluh, Z. Chen, Y. Li, K. Xiong, J. Jin, S. Fu, J. Wu, *Int J Nanomedicine* **2021**, 16, 2389.
- [37] A. Kulkarni, V. Chandrasekar, S. K. Natarajan, A. Ramesh, P. Pandey, J. Nirgud, H. Bhatnagar, D. Ashok, A. K. Ajay, S. Sengupta, *Nat. Biomed. Eng.* **2018**, 2, 589.
- [38] A. Ramesh, S. Kumar, D. Nandi, A. Kulkarni, *Adv. Mater.* **2019**, 31, 1904364.
- [39] A. Ramesh, A. Brouillard, S. Kumar, D. Nandi, A. Kulkarni, *Biomaterials* **2020**, 227, 119559.
- [40] A. Ramesh, V. Malik, H. A. Ranjani, H. Smith, A. A. Kulkarni, *Drug Deliv Transl Res* **2021**, 11, 2.
- [41] C. G. Palivan, R. Goers, A. Najer, X. Zhang, A. Car, W. Meier, *Chem. Soc. Rev.* **2016**, 45, 377.
- [42] S. Egli, M. G. Nussbaumer, V. Balasubramanian, M. Chami, N. Bruns, C. Palivan, W. Meier, *J. Am. Chem. Soc.* **2011**, 133, 4476.
- [43] S. Iqbal, M. Blenner, A. Alexander-Bryant, J. Larsen, *Biomacromolecules* **2020**, 21, 1327.
- [44] S. Matoori, J.-C. Leroux, *Mater. Horiz.* **2020**, 7, 1297.
- [45] L. Shi, J. Zhang, M. Zhao, S. Tang, X. Cheng, W. Zhang, W. Li, X. Liu, H. Peng, Q. Wang, *Nanoscale* **2021**, 13, 10748.
- [46] A. Shapouri-Moghaddam, S. Mohammadian, H. Vazini, M. Taghadosi, S. A. Esmaeili, F. Mardani, B. Seifi, A. Mohammadi, J. T. Afshari, A. Sahebkar, *J. Cell. Physiol.* **2018**, 233, 6425.
- [47] I. Elisia, H. B. Pae, V. Lam, R. Cederberg, E. Hofs, G. Krystal, *J. Immunol. Methods* **2018**, 452, 26.
- [48] K. A. Binnemars-Postma, H. W. Ten Hoopen, G. Storm, J. Prakash, *Nanomedicine (Lond)* **2016**, 11, 2889.
- [49] M. Sousa de Almeida, E. Susnik, B. Drasler, P. Taladriz-Blanco, A. Petri-Fink, B. Rothen-Rutishauser, *Chem. Soc. Rev.* **2021**, 50, 5397.
- [50] H. M. Rostam, P. M. Reynolds, M. R. Alexander, N. Gadegaard, A. M. Ghaemmaghami, *Sci. Rep.* **2017**, 7, 3521.
- [51] M. O. Oyewumi, A. Kumar, Z. Cui, *Expert Rev. Vaccines* **2010**, 9, 1095.
- [52] R. R. Shah, D. T. O'Hagan, M. M. Amiji, L. A. Brito, *Nanomedicine (Lond)* **2014**, 9, 2671.
- [53] Y. Liu, Y. Yin, L. Wang, W. Zhang, X. Chen, X. Yang, J. Xu, G. Ma, *J. Mater. Chem. B* **2013**, 1, 3888.
- [54] Z. Yue, Z. You, Q. Yang, P. Lv, H. Yue, B. Wang, D. Ni, Z. Su, W. Wei, G. Ma, *J. Mater. Chem. B* **2013**, 1, 3239.
- [55] H. Yue, L. Yuan, W. Zhang, S. Zhang, W. Wei, G. Ma, *J. Mater. Chem. B* **2018**, 6, 393.
- [56] Q. Wei, N. Shen, H. Yu, Y. Wang, Z. Tang, X. Chen, *Biomater. Sci.* **2020**, 8, 5666.
- [57] P. J. Murray, *Annu. Rev. Physiol.* **2017**, 79, 541.
- [58] P. P. Patwardhan, O. Surriga, M. J. Beckman, E. de Stanchina, R. P. Dematteo, W. D. Tap, G. K. Schwartz, *Clin. Cancer Res.* **2014**, 20, 3146.
- [59] V. Chitu, E. R. Stanley, *Curr. Opin. Immunol.* **2006**, 18, 39.
- [60] S. M. Pyonteck, L. Akkari, A. J. Schuhmacher, R. L. Bowman, L. Sevenich, D. F. Quail, O. C. Olson, M. L. Quick, J. T. Huse, V. Teijeiro, M. Setty, C. S. Leslie, Y. Oei, A. Pedraza, J. Zhang, C. W. Brennan, J. C. Sutton, E. C. Holland, D. Daniel, J. A. Joyce, *Nat. Med.* **2013**, 19, 1264.
- [61] I. De, M. D. Steffen, P. A. Clark, C. J. Patros, E. Sokn, S. M. Bishop, S. Litscher, V. I. Maklakova, J. S. Kuo, F. J. Rodriguez, L. S. Collier, *Cancer Res.* **2016**, 76, 2552.
- [62] K. Y. Sletta, O. Castells, B. T. Gjertsen, *Frontiers in Oncology* **2021**, 11, 654817.
- [63] S. Q. Qiu, S. J. H. Waaijer, M. C. Zwager, E. G. E. de Vries, B. van der Vegt, C. P. Schröder, *Cancer Treat. Rev.* **2018**, 70, 178.
- [64] X. Zheng, K. Turkowski, J. Mora, B. Brüne, W. Seeger, A. Weigert, R. Savai, *Oncotarget* **2017**, 8, 48436.
- [65] M. F. Sanmamed, L. Chen, *Cell* **2018**, 175, 313.
- [66] A.-L. Xia, Y. Zhang, J. Xu, X. J. Lu, *Frontiers in Immunology* **2019**, 10, 1719.
- [67] Z. Zhao, L. Zheng, W. Chen, W. Weng, J. Song, J. Ji, *J. Hematol. Oncol.* **2019**, 12, 126.
- [68] C. Li, J. Wang, Y. Wang, H. Gao, G. Wei, Y. Huang, H. Yu, Y. Gan, Y. Wang, L. Mei, H. Chen, H. Hu, Z. Zhang, Y. Jin, *Acta Pharm. Sin. B* **2019**, 9, 1145.
- [69] R. S. Riley, C. H. June, R. Langer, M. J. Mitchell, *Nat Rev Drug Discov* **2019**, 18, 175.
- [70] A. Goldman, A. Kulkarni, M. Kohandel, P. Pandey, P. Rao, S. K. Natarajan, V. Sabbisetti, S. Sengupta, *ACS Nano* **2016**, 10, 5823.
- [71] G. Lôbo, K. L. R. Paiva, A. L. G. Silva, M. M. Simões, M. A. Radicchi, S. N. Báó, *Pharmaceutics* **2021**, 13, 1167.
- [72] O. Rifaie-Graham, S. Ulrich, N. F. B. Galensowske, S. Balog, M. Chami, D. Rentsch, J. R. Hemmer, J. Read de Alaniz, L. F. Boesel, N. Bruns, *J. Am. Chem. Soc.* **2018**, 140, 8027.
- [73] H. Barosova, B. Drasler, A. Petri-Fink, B. Rothen-Rutishauser, *J Vis Exp* **2020**.